A Tight Bound on BER of MCIK-OFDM with Greedy Detection and Imperfect CSI

Luong, T. V., & Ko, Y. (2017). A Tight Bound on BER of MCIK-OFDM with Greedy Detection and Imperfect CSI. *IEEE Communications Letters*. https://doi.org/10.1109/LCOMM.2017.2747549

Published in:
IEEE Communications Letters

Document Version:
Peer reviewed version

Queen's University Belfast - Research Portal:
Link to publication record in Queen's University Belfast Research Portal

Publisher rights
© Copyright 2017 IEEE - All rights reserved. This work is made available online in accordance with the publisher's policies. Please refer to any applicable terms of use of the publisher.

General rights
Copyright for the publications made accessible via the Queen's University Belfast Research Portal is retained by the author(s) and / or other copyright owners and it is a condition of accessing these publications that users recognise and abide by the legal requirements associated with these rights.

Take down policy
The Research Portal is Queen's institutional repository that provides access to Queen's research output. Every effort has been made to ensure that content in the Research Portal does not infringe any person's rights, or applicable UK laws. If you discover content in the Research Portal that you believe breaches copyright or violates any law, please contact openaccess@qub.ac.uk.

Download date:05. May. 2023

A Tight Bound on BER of MCIK-OFDM with Greedy Detection and Imperfect CSI

Thien Van Luong, *Student Member, IEEE,* and Youngwook Ko, *Member, IEEE*

***Abstract*—This letter first investigates bit error rate (BER) of Multi-Carrier Index Keying - Orthogonal Frequency Division Multiplexing (MCIK-OFDM) using a low-complexity greedy detector (GD). We derive a tight, closed-form expression for the BER of the GD in the presence of channel state information (CSI) uncertainty. Particularly, exploiting the fact that the GD detects the active indices first, and then detects the data symbols, we divide the BER into two terms: the index BER and the symbol BER. The asymptotic analysis is also provided to analyze impacts of various CSI conditions on the BER. Interestingly, via theoretical and simulation results, we discover that the GD is not only less sensitive to imperfect CSI, but also better than the maximum likelihood detector under certain CSI conditions. In addition, the derived expression is accurate in a wide range of signal-to-noise ratio regions.**

***Index Terms*—MICK-OFDM, OFDM-IM, greedy detector, index modulation, bit error rate, imperfect CSI.**

I. Introduction

Multi-Carrier Index Keying - Orthogonal Frequency Division Multiplexing (MCIK-OFDM) or the so-called OFDM with Index Modulation (OFDM-IM) [1] has recently emerged as a promising multicarrier technique due to its higher spectral and energy efficiency over the classical OFDM. In MCIK-OFDM, only a fraction of sub-carriers are activated to convey data bits via both the M-ary modulated symbols and the indices of active sub-carriers. Thus, MCIK-OFDM can provide an attractive trade-off between reliability and spectral efficiency by adjusting the number of active sub-carriers.

Recently, MCIK-OFDM has received significant attention from researchers, as presented in the surveys [2], [3]. Note that most of existing studies focus on the bit error rate (BER) analysis of MCIK-OFDM considering the maximum likelihood (ML) detector [4], [5]. Meanwhile, in [6], a low-complexity greedy detector (GD) is proposed, which employs energy detection in the index detection without the need of channel state information (CSI). Very recently, the pairwise error probability (PEP) and symbol error probability (SEP) of the GD are analyzed in [7], [8]. However, these studies only consider the perfect CSI case, thus the expected robustness of the GD to imperfect CSI has not been investigated. Moreover, to the best of our knowledge, the BER of the GD has not been explored in the literature yet.

In this letter, we first derive a tight closed-form expression for the BER of a generalized MCIK-OFDM with the GD under uncertain CSI. In particular, motivated by the fact that the first step, i.e., the index detection in the GD is independent of the second step (M-ary symbol detection) [6], we separately analyze the index BER (IBER) and the symbol BER (SBER) to obtain the overall BER. In addition, to gain an insight into impacts of uncertain CSI, the asymptotic analysis on the BER are presented. Finally, simulation results validate the accuracy of our derived expression and the much better resistance of the GD to uncertain CSI over the ML.[1]

II. System Model

A. MCIK-OFDM

Consider an MCIK-OFDM system consisting of N_c sub-carriers, which is divided into G clusters. Each cluster has N sub-carriers, i.e., $N_c = NG$. For every transmission, only K out of N sub-carriers are active to carry data symbols, while $N-K$ remaining sub-carriers keep idle. At the transmitter, a total of p bits enter each cluster, which then are partitioned into two bit streams ($p = p_1 + p_2$). The first p_1 bits are mapped to a corresponding set of K active indices, using look-up table (LUT) or combinatorial method [1]. Denote this set by $\theta = \{\alpha_1, ..., \alpha_K\}$, where $\alpha_k \in \{1, ..., N\}$ for $k = 1, ..., K$. Note that θ is considered as an index symbol, which is determined by p_1 index bits. For given N, K, the number of index bits is given by $p_1 = \lfloor \log_2 C(N, K) \rfloor$. The second p_2 bits are mapped to K complex M-ary symbols, thus $p_2 = K \log_2 M$. Based on the active index set θ and K symbols, the transmitted vector is generated as $\mathbf{x} = [x(1), ..., x(N)]^T$, where $x(\alpha) \in \mathcal{S}$ for $\alpha \in \theta$ and $x(\alpha) = 0$ for $\alpha \notin \theta$, $\alpha = 1, ..., N$. Here, $\mathcal{S}$ denotes the M-ary constellation.

The received signal in the frequency domain is given by

$$\mathbf{y} = \mathbf{H}\mathbf{x} + \mathbf{n}, \tag{1}$$

where the channel matrix $\mathbf{H} = \text{diag}\{h(1), ..., h(N)\}$ has its entries being complex Gaussian random variables with zero mean and unit variance, i.e., $h(\alpha) \sim \mathcal{CN}(0, 1)$, and $\boldsymbol{n}$ denotes the additive white Gaussian noise (AWGN) vector with $n(\alpha) \sim \mathcal{CN}(0, N_0)$. Assume that each non-zero symbol has the average transmit power of φE_s, where $\varphi = N/K$ is the power allocation coefficient and E_s is the average power per sub-carrier. Thus, the average signal-to-noise ratio (SNR) per active sub-carrier is given by $\bar{\gamma} = \varphi E_s / N_0$.

B. GD Detection under Imperfect CSI

In a practical system, the CSI is imperfectly known at the receiver. In particular, the channel estimate for each sub-carrier (denoted by $\hat{h}(\alpha)$) is given by

$$\hat{h}(\alpha) = h(\alpha) - e(\alpha), \tag{2}$$

[1]Upper and lower case boldface letter denote matrices and column vectors, respectively. $C(.,.)$ denotes the binomial coefficient. $(.)^T$ and $\lfloor . \rfloor$ stand for transpose and floor operations, respectively. $\mathcal{CN}(0, \sigma^2)$ denotes the circularly symmetric complex Gaussian distribution with zero mean and variance σ^2.

where $e(\alpha) \sim \mathcal{CN}(0, \epsilon^2)$ denotes the channel estimation error, where ϵ^2 is the CSI error variance. Assume that $\hat{h}(\alpha)$ and $e(\alpha)$ are independent, which leads to $\hat{h}(\alpha) \sim \mathcal{CN}(0, 1-\epsilon^2)$.

The GD decodes signals in the presence of $\hat{h}(\alpha)$, via two steps as follows. First, K active indices (denoted by $\hat{\theta} = \{\hat{\alpha}_1, ..., \hat{\alpha}_K\}$) are detected by the corresponding K sub-carriers which have largest received energy. Then, M-ary symbols are retrieved by using the ML decision per active sub-carrier detected, as

$$\hat{x}(\hat{\alpha}) = \arg \min_{x(\hat{\alpha}) \in \mathcal{S}} \left| y(\hat{\alpha}) - \hat{h}(\hat{\alpha}) x(\hat{\alpha}) \right|^2. \quad (3)$$

It is noteworthy that the GD offers a significantly reduced complexity compared to the ML, at the acceptable loss of reliability. Moreover, since the GD employs energy detection in the index recovery process without the need of CSI, this detector is expected to less sensitive to CSI uncertainty than the ML. This will be investigated in the next sections.

III. BER Analysis with Imperfect CSI

As mentioned above, the GD separately detects the indices and M-ary symbols via two steps, where the first step does not depend on the second. Whereas, the M-ary symbol detection in the second step is strongly affected by the accuracy of the index detection in the first step. This interesting feature of the GD motivates us to divide the bit error event into two types: the index bit error (p_1 bits) and the symbol bit error (p_2 bits). Specifically, denote by P_1 and P_2 the IBER and the SBER, respectively, the BER of the GD can be expressed as

$$P_b = \frac{p_1 P_1 + p_2 P_2}{p_1 + p_2}. \quad (4)$$

Thus, to evaluate the BER, we now analyze P_1 and P_2 as follows.

A. Index Bit Error Rate

Notice that the IBER can be obtained based on the index error probability (IEP) that θ is inaccurately detected. Denote by P_I the instantaneous IEP, which can be given as [7]

$$P_I \leq \frac{K}{N} \sum_{\alpha=1}^{N} P_I(\alpha), \quad (5)$$

where K/N is the probability that sub-carrier α is activated at the transmitter, and $P_I(\alpha)$ denotes the probability that sub-carrier α is incorrectly detected as an inactive one. $P_I(\alpha)$ can be written by

$$P_I(\alpha) \leq \sum_{\tilde{\alpha} \neq \alpha = 1}^{N-K} P(\alpha \to \tilde{\alpha}), \quad (6)$$

where $P(\alpha \to \tilde{\alpha})$ denotes the pairwise error probability (PEP), that activated sub-carrier α is inaccurately decoded as inactive sub-carrier $\tilde{\alpha} \neq \alpha$.

Using (5)-(6), the IEP of the GD can be obtained by [6], [8]

$$P_I \leq \frac{K}{N} \sum_{\alpha=1}^{N} \sum_{i=1}^{N-K} \frac{(-1)^{i+1} C(N-K, i)}{i+1} e^{-\frac{i\bar{\gamma}\nu_\alpha}{i+1}}, \quad (7)$$

where $\nu_\alpha = |h(\alpha)|^2$. Interestingly, as seen from (7), P_I is independent of imperfect CSI, i.e., $\hat{h}(\alpha)$. Due to system model, the moment generating function (MGF) of ν_α is given by $\mathcal{M}_\nu(s) = (1-s)^{-1}$. Consequently, using the MGF approach to (7), the average IEP is attained as

$$\overline{P}_I \leq K \sum_{i=1}^{N-K} \frac{(-1)^{i+1} C(N-K, i)}{i+1+i\bar{\gamma}}. \quad (8)$$

For the special case with $(N, K) = (2, 1)$, there are two possible index symbols ($p_1 = 1$), thus we obtain $P_1 = \overline{P}_I$. For $N > 2$ and $K < N$, notice that the mapping rules between index bits and active indices such as LUT and combinatorial method [1] do not provide Gray codes. For example, MCIK-OFDM with $(N, K) = (4, 1)$, we have four index symbols as $\theta_i = \{i\}$, for $i = 1, ..., 4$. It can be seen that the PEPs that θ_i is incorrectly detected as $\theta_j \neq \theta_i$ are the same for any $j \neq i$. That means for given i, there is no such PEP that becomes dominant over the others. Based on this observation, the IBER can be approximated as $P_1 \approx \overline{P}_I/2$ for $N > 2$. For convenience, we represent the IBER as follows

$$P_1 \approx \eta \overline{P}_I/2, \quad (9)$$

where $\overline{P}_I$ is given in (8), $\eta = 1, 2$ for $N > 2$ and $N = 2$, respectively.

It is noteworthy from (9) that the IBER expression of the GD is independent of both ϵ^2 and M.

B. Symbol Bit Error Rate

For transmitted data symbol $x(\alpha)$, because the ML-based detection of this symbol depends on the index detection error, we consider two following symbol error cases. In case the index α is correctly detected, the probability of the misdetection of $x(\alpha)$ equals the M-ary SEP, which is denoted by $P_M(\alpha)$. This results in the instantaneous SBER corresponding to $x(\alpha)$ being $P_M(\alpha)/\log_2 M$, when the Gray mapping is used. By contrast, if α is inaccurately decoded, $x(\alpha)$ will be estimated without any CSI knowledge. In this case, the instantaneous SBER for $x(\alpha)$ will be $1/2$. Therefore, using the total probability theory, we attain the instantaneous SBER (denoted by iP_2) as

$$iP_2 \leq \frac{1}{N} \sum_{\alpha=1}^{N} \left[\frac{P_I(\alpha)}{2} + (1 - P_I(\alpha)) \frac{P_M(\alpha)}{\log_2 M} \right]. \quad (10)$$

Inserting (5) and (6) into (10), and using the fact that $1 - P_I(\alpha) \leq 1$, we get

$$iP_2 \leq \frac{P_I}{2K} + \frac{1}{mN} \sum_{\alpha=1}^{N} P_M(\alpha), \quad (11)$$

where $m = \log_2 M$. Hence, the SBER of the GD can be obtained by taking expectation of (11) as

$$P_2 \leq \frac{\overline{P}_I}{2K} + \frac{\overline{P}_M}{m}, \quad (12)$$

where $\overline{P}_M$ denotes the average of $P_M(\alpha)$.

We assume the M-ary PSK modulation is used, and the corresponding $\overline{P}_M$ is given in the following lemma.

Lemma 1. *Under CSI imperfection with the error variance ϵ^2, the average SEP of conventional M-ary PSK symbols is approximated by*

$$\overline{P}_M \approx \frac{\xi}{12}\left[\frac{1}{1+\frac{(1-\epsilon^2)\bar{\gamma}\rho}{1+\bar{\gamma}\epsilon^2}}+\frac{3}{1+\frac{4(1-\epsilon^2)\bar{\gamma}\rho}{3+3\bar{\gamma}\epsilon^2}}\right], \tag{13}$$

where $\xi = 1, 2$ for $M = 2$ and $M > 2$, respectively and $\rho = \sin^2(\pi/M)$.

Proof: See Appendix A. ∎

Finally, substituting (8) and (13) into (12), we obtain the SBER of the GD under CSI uncertainty, in closed-form as

$$P_2 \leq \frac{1}{2}\sum_{i=1}^{N-K}\frac{(-1)^{i+1}C(N-K,i)}{i+1+i\bar{\gamma}} + \frac{\xi}{12m}\left[\frac{1}{1+\frac{(1-\epsilon^2)\bar{\gamma}\rho}{1+\bar{\gamma}\epsilon^2}}+\frac{3}{1+\frac{4(1-\epsilon^2)\bar{\gamma}\rho}{3+3\bar{\gamma}\epsilon^2}}\right]. \tag{14}$$

As shown in (14), the SBER strongly depends on the index detection error (via the first term), especially when M is small.

C. BER of GD Detector with Uncertain CSI

The expression for the BER of the GD under imperfect CSI, can be obtained by substituting (9) and (14) into (4) as follows

$$P_b \approx \frac{K(\eta p_1+m)}{2p}\sum_{i=1}^{N-K}\frac{(-1)^{i+1}C(N-K,i)}{i+1+i\bar{\gamma}} + \frac{K\xi}{12p}\left[\frac{1}{1+\frac{(1-\epsilon^2)\bar{\gamma}\rho}{1+\bar{\gamma}\epsilon^2}}+\frac{3}{1+\frac{4(1-\epsilon^2)\bar{\gamma}\rho}{3+3\bar{\gamma}\epsilon^2}}\right], \tag{15}$$

where we recall that $p = p_1 + p_2$ and $p_2 = K\log_2 M = Km$.

As observed from (15), ϵ^2 only appears in the term related to the M-ary symbol detection in the second step of the GD. Hence, the BER of MCIK-OFDM with the GD can be less sensitive to CSI uncertainty than the ML. In addition, our derivation is also valid for M-QAM modulation with $\rho = 1.5/(M-1)$ [9] since the IBER of the GD does not depend on M as shown in (9).

IV. Asymptotic Analysis

We now asymptotically analyze the BER of MCIK-OFDM with the GD at high SNRs. This provides an insight into impacts of various CSI conditions such as perfect, fixed and minimum mean square error (MMSE)-based variable CSI.

A. Perfect CSI ($\epsilon^2 = 0$)

As $\bar{\gamma}$ is very large and $\epsilon^2 = 0$, the BER in (15) can be asymptotically approximated by

$$P_b \approx \frac{K^2}{2pN}\left[\omega(\eta p_1+m)+\frac{13\xi}{24\rho}\right]\left(\frac{1}{\gamma_0}\right), \tag{16}$$

where $\omega = \sum_{i=1}^{N-K}(-1)^{i+1}C(N-K,i)/i$ and γ_0 denotes the average SNR per sub-carrier, i.e., $\gamma_0 = E_s/N_0$.

As seen from (16), under perfect CSI, the GD achieves diversity order of one. In addition, for given N and M, the BER becomes better as K gets smaller.

B. Fixed CSI Uncertainty ($\epsilon^2 > 0$)

For given $\epsilon^2 > 0$, (15) can be rewritten at high SNRs as

$$P_b \approx \frac{K\xi}{12p}\left[\frac{1}{1+\frac{(1-\epsilon^2)\rho}{\epsilon^2}}+\frac{3}{1+\frac{4(1-\epsilon^2)\rho}{3\epsilon^2}}\right], \tag{17}$$

which is no longer a function of the SNR.

It is shown from (17) that there exists an error floor on the BER of the GD, which is given only by the term $\overline{P}_M$. In other words, increasing SNR does not improve the BER performance in this case. Furthermore, for given N, the error floor gets higher as K gets larger. And, for given K, as N increases, the error floor becomes lower.

C. MMSE-Based Variable CSI Uncertainty

The MMSE channel estimator yields the error variance that varies as a decreasing function of γ_0, which is

$$\epsilon^2 = \frac{1}{1+E_s/N_0}. \tag{18}$$

The proof of (18) is presented in Appendix A.

Plugging (18) into (15), at high SNR, we obtain the asymptotic BER as

$$P_b \approx \frac{K}{2pN}\left[K\omega(\eta p_1+m)+\frac{13\xi(N+K)}{24\rho}\right]\left(\frac{1}{\gamma_0}\right). \tag{19}$$

Compared to the perfect CSI case, the BER in this case still has the diversity order of one, however, suffers from a loss of coding gain given as follows

$$\Delta = 10\log\left[\frac{\omega(\eta p_1+m)+\frac{13\xi}{24\rho}\left(1+\frac{N}{K}\right)}{\omega(\eta p_1+m)+\frac{13\xi}{24\rho}}\right] \text{(dB)}. \tag{20}$$

It can be seen in (20), the loss Δ gets smaller as K increases for given N.

V. Simulation Results

The simulation results are presented for various MCIK-OFDM schemes to verify the derived expressions, under different CSI uncertainties. We consider the Rayleigh fading per sub-carrier. The simulation results for the ML detector are used for comparison.

Fig. 1 shows the BERs of both the GD and the ML under three CSI conditions, when $(N, K, M) = (2, 1, 2)$. As seen via this figure, our derived theoretical bounds for the BER of the GD are accurate in almost SNR regions, even at very low SNRs. The loss of SNR gain caused by MMSE variable CSI with the GD is less than 1 dB, which is much smaller than that of the ML (about 5 dB). This clearly indicates that the GD is far less sensitive to CSI uncertainty than the ML. Moreover, for fixed CSI ($\epsilon^2 = 0.02$), the GD even provides the optimal performance at high SNRs like the ML, at a much lower complexity. Note that this interesting robustness of the GD to CSI imperfection has not seen in the literature.

Fig. 2 depicts the BERs of MCIK-OFDM with $(N, K, M) = (4, 1, 4)$ and two detectors. As observed in Fig. 2, under perfect CSI, the performance gap between the GD and the ML is 5 dB at BER of 10^{-3}. However, this

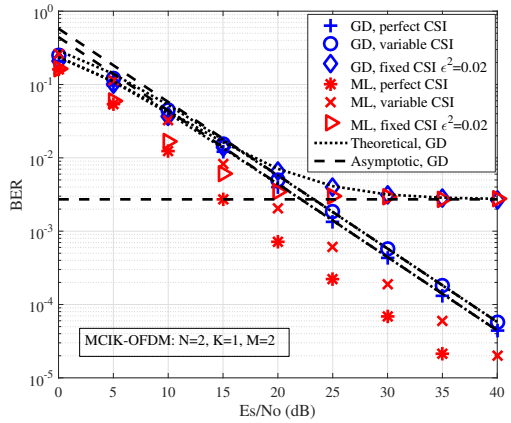

Fig. 1. BER performance of MCIK-OFDM using GD and ML under various CSI conditions, when $N = 2,\ K = 1,\ M = 2$.

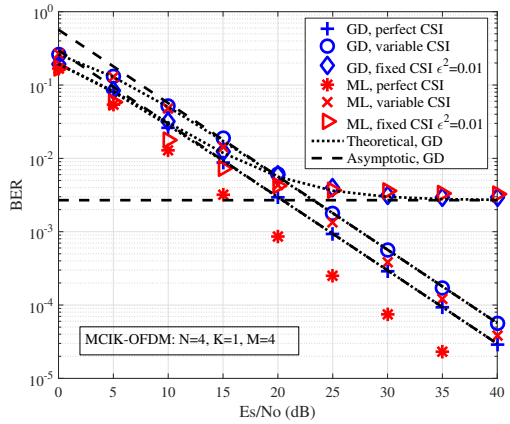

Fig. 2. BER performance of MCIK-OFDM using GD and ML under various CSI conditions, when $N = 4,\ K = 1,\ M = 4$.

gap becomes much smaller under MMSE variable CSI, with only about 1 dB. Under fixed CSI, the GD even slightly outperforms the ML. Thus, we can see that the GD is preferred to the ML in the presence of CSI uncertainty due to its competitive BER performance and complexity. Finally, this figure also validates the tightness of the BER expression of the GD in whole SNR regions.

VI. Conclusions

Utilizing the principle of the low-complexity GD detector in MCIK-OFDM, we have derived a tight bound on the BER of this detector in the presence of CSI uncertainty. This allows to provide an insight into impacts of various CSI conditions on the BER of the GD in MCIK-OFDM systems. Interestingly, our analysis clearly showed that the GD is not only far less sensitive to imperfect CSI, but also able to have a better BER than the ML in some uncertain CSI cases.

Appendix A
Proofs of Lemma1 and (18)

Proof of Lemma 1: Using (1) and (2), we have $y(\alpha) = x(\alpha)\hat{h}(\alpha) + \tilde{n}(\alpha)$, where $\tilde{n}(\alpha) = x(\alpha)e(\alpha) + n(\alpha)$ is the noise caused by both AWGN and CSI imperfection, and $\tilde{n}(\alpha) \sim \mathcal{CN}\left(0, N_0 + \varphi E_s\epsilon^2\right)$. Thus, provided that the index α is correctly detected, the second step of the GD will detect $x(\alpha)$ with an instantaneous SNR of $\hat{\gamma}_\alpha = \varphi E_s \left|\hat{h}(\alpha)\right|^2 / \left(N_0 + \varphi E_s\epsilon^2\right) = \bar{\gamma}\hat{\nu}_\alpha / \left(1 + \bar{\gamma}\epsilon^2\right)$, where $\hat{\nu}_\alpha = \left|\hat{h}(\alpha)\right|^2$. Note that $P_M(\alpha)$ can be approximated as [9],

$$P_M(\alpha) \approx \xi Q\left[\sqrt{\hat{\gamma}_\alpha}\sin\left(\frac{\pi}{M}\right)\right], \tag{21}$$

where $\xi = 1$ for $M = 2$ and $\xi = 2$ for $M > 2$. From (21), $P_M(\alpha)$ can be rewritten, using the approximation of Q-function $Q(x) \approx \frac{1}{12}e^{-x^2/2} + \frac{1}{4}e^{-2x^2/3}$, as

$$P_M(\alpha) \approx \frac{\xi}{12}\left(e^{-\hat{\gamma}_\alpha\rho} + 3e^{-\frac{4\hat{\gamma}_\alpha\rho}{3}}\right), \tag{22}$$

where $\rho = \sin^2(\pi/M)$.

Using MGF approach to (22), with the MGF of $\hat{\nu}_\alpha$ given by $\mathcal{M}_{\hat{\nu}}(z) = \left[1 - \left(1 - \epsilon^2\right)z\right]^{-1}$, the average SEP of the M-ary PSK symbols is attained as (13). This concludes the proof.

Proof of (18)*:* Assume that the transmit power of the pilots $x_p(\alpha) = 1$ for $\alpha = 1, ..., N$ equals the average transmit power per sub-carrier, i.e., E_s. The received pilot signal is $y(\alpha) = \sqrt{E_s}h(\alpha) + n(\alpha)$. Using MMSE principle, $\hat{h}(\alpha)$ is estimated as

$$\begin{aligned}\hat{h}(\alpha) &= \frac{y(\alpha)\,\mathbb{E}\left\{y(\alpha)\,h^*(\alpha)\right\}}{\mathbb{E}\left\{\left|y(\alpha)\right|^2\right\}} \\ &= \frac{\sqrt{E_s}}{E_s + N_0}\left[\sqrt{E_s}h(\alpha) + n(\alpha)\right].\end{aligned} \tag{23}$$

Thus, due to $e(\alpha) = h(\alpha) - \hat{h}(\alpha)$, we obtain

$$e(\alpha) = \frac{N_0}{E_s + N_0}h(\alpha) - \frac{\sqrt{E_s}}{E_s + N_0}n(\alpha). \tag{24}$$

Because $h(\alpha)$ and $n(\alpha)$ are independent, based on (24), the error variance of $e(\alpha)$ can be obtained as in (18).

Acknowledgment

This work was supported by the Engineering and Physical Sciences Research Council [grant number EP/N509541/1].

References

[1] E. Basar, U. Aygolu, E. Panayirci, and H. V. Poor, "Orthogonal frequency division multiplexing with index modulation," *IEEE Trans. Signal Process.*, vol. 61, no. 22, pp. 5536–5549, Nov 2013.

[2] N. Ishikawa, S. Sugiura, and L. Hanzo, "Subcarrier-index modulation aided OFDM - will it work?" *IEEE Access*, vol. 4, pp. 2580–2593, 2016.

[3] E. Basar, "Index modulation techniques for 5G wireless networks," *IEEE Commun. Mag.*, vol. 54, no. 7, pp. 168–175, July 2016.

[4] Y. Ko, "A tight upper bound on bit error rate of joint OFDM and multi-carrier index keying," *IEEE Commun. Lett.*, vol. 18, no. 10, pp. 1763–1766, Oct 2014.

[5] J. Choi, "Coded OFDM-IM with transmit diversity," *IEEE Trans. Commun.*, vol. PP, no. 99, pp. 1–1, 2017.

[6] J. Crawford and Y. Ko, "Low complexity greedy detection method with generalized multicarrier index keying OFDM," in *Proc. IEEE Pers., Indoor., Mobile Radio Commun.*, Aug 2015, pp. 688–693.

[7] E. Chatziantoniou, J. Crawford, and Y. Ko, "Performance analysis of a low-complexity detector for MCIK-OFDM over TWDP fading," *IEEE Commun. Lett.*, vol. 20, no. 6, pp. 1251–1254, June 2016.

[8] J. Crawford, E. Chatziantoniou, and Y. Ko, "On the SEP analysis of OFDM index modulation with hybrid low complexity greedy detection and diversity reception," *IEEE Trans. Veh. Technol.*, vol. PP, no. 99, pp. 1–1, 2017.

[9] J. Proakis, *Digital Communications*, ser. Electrical engineering series. McGraw-Hill, 2001.